

Percolative Behavior of the Superconductive Transition of $\text{YBa}_2\text{Cu}_3\text{O}_7$ Films

Ch. Leemann, Ph. Flückiger, V. Marsico, J. L. Gavilano,^(a) P. K. Srivastava, Ph. Lerch, and P. Martinoli

Institut de Physique, Université de Neuchâtel, 2000 Neuchâtel, Switzerland

(Received 30 March 1990)

The superconductive transition of *c*-axis-oriented $\text{YBa}_2\text{Cu}_3\text{O}_7$ thin films, as characterized by measurements of the temperature dependence of the magnetic penetration depth, is found to occur below the Ginzburg-Landau mean-field transition. The divergence of the penetration depth at the transition is in good quantitative agreement with the predictions of a percolation model.

PACS numbers: 74.50.+r, 74.70.Mq

Scanning electron micrographs of high-temperature superconducting ceramics create the impression of a conglomerate of grains of size $\sim 1 \mu\text{m}$, thereby requiring the necessity to incorporate granularity in the description of these materials and their physical properties. Coupled with the knowledge of a pathologically short coherence length, of the order of 10 \AA ,¹ which in no way can smooth out the grainy structure, this leads quite naturally to modeling these ceramics as networks of grains coupled by Josephson weak links.^{2,3} Of course such a picture does not preclude the existence of intrinsic weak-link effects within the material itself, as postulated by Deutscher and Müller,⁴ which are, however, if at all, only observable with the utmost care and precaution in single-crystal samples. Under normal circumstances the strength (or weakness) of the grain-to-grain coupling is expected to play a dominant role in determining macroscopic transport properties. In this paper we present measurements of the penetration depth in two-dimensional (2D), *c*-axis-oriented $\text{YBa}_2\text{Cu}_3\text{O}_7$ (YBCO) films. These measurements are in excellent agreement with a percolation description of the films, based on the assumptions that the grains are coupled via the usual Ambegaokar-Baratoff⁵ tunnel-junction formula and that the normal-state junction resistances R_n obey a Gaussian distribution. The characteristic features of 2D critical fluctuations in the form of a Kosterlitz-Thouless-Berezinski (KTB) vortex unbinding transition,⁶ in principle present and observed in some cases,⁷⁻¹⁰ are completely masked by the much more prominent consequences of random coupling between the grains.

Thin films of YBCO were deposited onto polished SrTiO_3 (100) substrates with an *in situ* (no annealing) process using cylindrical "hollow cathode" magnetron single-target sputtering.¹¹ After some fine tuning, this method was found to produce superior quality films. The transport critical current density in these films increases sharply below the mean-field transition temperature T_{c0} , to reach 10^6 A/cm^2 at, typically, a reduced temperature $T/T_{c0} \approx 0.8$. In the following we will consider one representative film of thickness $d \sim 200 \text{ \AA}$ as determined by Rutherford backscattering spectrometry. X-ray analysis showed that the film was *c*-axis oriented. The effective thin-film penetration depth $\Lambda = 2\lambda^2/d$, where λ

is the bulk in-plane penetration depth, was deduced from measurements of the film's screening properties.^{12,13} The film is positioned directly underneath a cylindrical excitation coil and a coaxial gradiometer detection coil. A current flowing in the excitation coil induces screening currents in the film which in turn induce a signal in the detection coil. From this signal, measured phase sensitively, the complex sample impedance $Z = R + i\omega L_k$ can be extracted¹³ and thus Λ from the sheet kinetic inductance L_k , since $\Lambda = 2L_k/\mu_0$. In Fig. 1 the in-phase, $\text{Re}\delta V$, and quadrature, $\text{Im}\delta V$, components of the signal voltage measured at a frequency of 3 kHz are shown as a function of temperature, and, on a different temperature scale but with a common point at 79 K, the result of a four-probe van der Pauw measurement of the dc resistive transition. For these measurements, the ambient magnetic field was reduced to $\sim 1 \text{ mG}$ with Mu-metal shielding. The relatively low T_{c0} (79 K) is probably caused by the thinness of the film; thicker films ($d \geq 1000 \text{ \AA}$) prepared with the same processing method had, typically, a T_{c0} of 90 K. The choice of such a thin film was dictated by the need to increase Λ in order to improve the

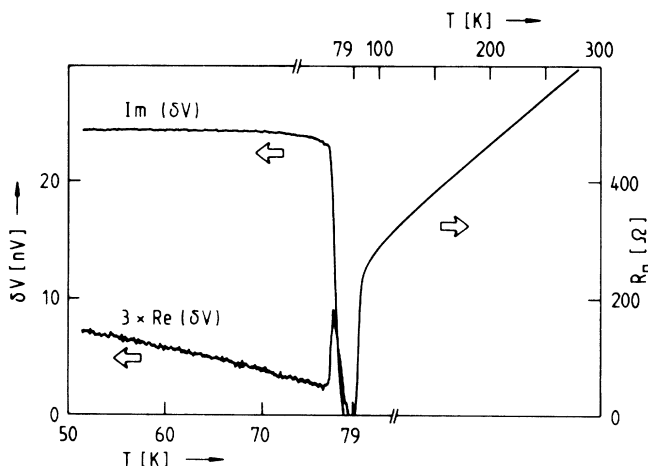


FIG. 1. Real, $\text{Re}\delta V$, and imaginary, $\text{Im}\delta V$, parts of the signal voltage measured at 3 kHz and the sheet resistance as a function of temperature. Note the different temperature scales for the resistive and inductive data, with a common point at $T = 79 \text{ K}$.

measurement sensitivity. Notice that the inductive response starts with the sheet resistance $R_0 \approx 0$, and that the $\text{Re}\delta V(T)$ component, characterized by a peak at the transition, exhibits a low-temperature tail not normally observed in such measurements.¹³ In Fig. 2 the result of the analysis outlined above, applied to the measurement of Fig. 1, is shown together with the dc resistive transition on the same temperature scale. The temperature dependence of Λ^{-1} is linear below ~ 75 K and there is a "jump" to zero setting in at ~ 76 K. Except very close to T_{c0} , the screening properties of the film were found to be quite insensitive to weak (up to 0.5 T) magnetic fields. Together with the sharpness of both the resistive and inductive transitions, this demonstrates the good quality of this very thin film.

While the film's properties presented above demonstrate that it certainly is not a system of loosely coupled grains, we nonetheless assume that, at least in the transition region, granularity is the key feature. Accordingly, for the interpretation of the temperature dependence of Λ^{-1} presented in Fig. 2, we follow the basic ideas set forth by Deutscher *et al.*¹⁴ and Ebner and Stroud.¹⁵ All the individual grains in the film become superconducting at the same temperature T_{c0} ; however, two grains are coupled only when the Josephson coupling energy E_J exceeds the thermal energy kT . Charging effects are neglected: The high transition temperature, the relatively large grain size and the not exceedingly large junction resistance guarantee that, at least in the transition region, the charging energy $E_c \ll kT$. Then, if the coupling between the grains follows some statistical distribution function, the superconducting transition becomes a bond percolation problem. As the temperature is lowered, the

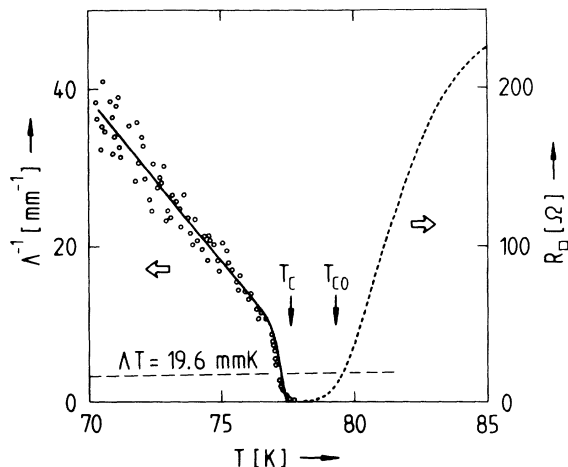


FIG. 2. Temperature dependence (circles) of Λ^{-1} deduced from the measurement of Fig. 1 and (solid line) the fit for Λ^{-1} according to Eq. (7). The dotted line above T_c is the resistive transition. T_{c0} is given by the extrapolation to zero of the linear part of Λ^{-1} ; T_c was determined from the fit and Eq. (6). The dashed line is the Kosterlitz-Thouless prediction $\Lambda(T_c)T_c = 19.6$ mm K.

fraction p of coupled grains increases, the exact functional relationship $p(T)$ being determined by the choice of the independent random variable and its distribution function. Since in our experiments we measure $\Lambda(T)$, in order to interpret the measurements in terms of a percolation model, an expression for $\Lambda(p(T))$ is necessary. In Ref. 15 the helicity modulus Γ (proportional to the superfluid density and hence to Λ^{-1}) in a three-dimensional (3D) site-diluted granular superconductor was shown to be proportional to the normal-state conductivity σ :

$$\Gamma(p)/\Gamma(1) = \sigma(p)/\sigma(1). \quad (1)$$

The grain size being of the order of $1 \mu\text{m}$ and the film thickness $\sim 200 \text{ \AA}$, the percolation dimensionality is 2. The validity of Eq. (1) was demonstrated by showing that, at a given percolation probability, the superfluid density is proportional to the conductance of the sample in the normal state.¹⁵ It appears reasonable to assume that this result, and therefore Eq. (1), is true in 2D as well as 3D. A further *caveat* concerning Eq. (1) should be mentioned: It is valid only at low temperatures, below the critical region where fluctuations in the phase of the superconducting order parameter renormalize Γ . As we will see, the percolative transition occurs below this critical temperature regime in our samples. The use of Eq. (1) appears thus to be justified and we expect Λ to diverge with the conductivity exponent t :¹⁶

$$\Lambda(p) = \Lambda(1) \frac{1}{|p - p_c|^t}, \quad (2)$$

where p_c is the percolation threshold.

For the derivation of $p(T)$, we assume that the normal-state grain-grain resistances R_n obey a Gaussian centered at R_{av} , with standard deviation δR . The junction coupling energy is given by⁵

$$E_J = \frac{h}{8e^2 R_n} \Delta(T) \tanh \frac{\Delta(T)}{2kT}, \quad (3)$$

an expression applicable not only to tunnel junctions, but also, e.g., to metallic weak links.¹⁷ Since everything of interest happens close to T_{c0} , we expand the gap parameter $\Delta(T)$ and the tanh function to find

$$E_J = \frac{R_0}{R_n} k\delta T \quad (4)$$

valid for $\delta T \equiv T_{c0} - T \ll T_{c0}$, with $R_0 = 3.7\hbar/e^2$. The condition for superconducting coupling between two grains $E_J \geq kT$ now reduces to $R_n \leq R_0 \delta T/T$. The fraction of grain-grain resistances less than R_n being given by $\text{erf}[(R_n - R_{av})/\delta R]$, where

$$\text{erf}(x) \equiv \frac{1}{\sqrt{2\pi}} \int_{-\infty}^x e^{-y^2/2} dy,$$

we arrive at the result

$$p(T) = \text{erf} \left[\frac{R_0 \delta T/T - R_{av}}{\delta R} \right]. \quad (5)$$

Zero resistance is reached when $\rho(T) = p_c$, a condition which, for $p_c = 0.5$, results in a temperature T_c given by

$$T_c = T_{c0} \frac{R_0}{R_0 + R_{av}} \approx T_{c0} \left(1 - \frac{R_{av}}{R_0} \right), \quad (6)$$

since $R_{av} \ll R_0$. With a slightly different R_0 value, this is the same relationship for the reduction of T_c as in a superconducting film undergoing a KTB transition.¹⁸ The final result for the temperature dependence of Λ is thus

$$\Lambda(T) = \frac{\Lambda(0)}{2(1 - T/T_{c0})} \frac{p_0}{|p(T) - p_c|^t}, \quad (7)$$

where $p_0 = |p(0) - p_c|^t$ ensures the consistency of the equation at $T=0$, and $p(T)$ is given by Eq. (5). Since in YBCO the mean free path is larger than the coherence length, we have used the clean limit expression for $\Lambda(T)$ in the Ginzburg-Landau regime,¹⁹ leading to the factor of 2 in the denominator of Eq. (7).

The solid line in Fig. 2 is a numerical calculation of $\Lambda^{-1}(T)$ with Eqs. (5), (7), and the explicit expression for $\text{erf}(x)$ given above. The fitting parameters $\Lambda(0) = 6.0 \mu\text{m}$ and $T_{c0} = 79.3 \text{ K}$ are determined by the straight, low-temperature section of the curve. The two arrows in Fig. 2 indicate the temperatures T_{c0} and $T_c = 77.4 \text{ K}$, as determined with Eq. (6). The $\Lambda(0)$ value corresponds to $\lambda(0) = 0.24 \mu\text{m}$, a zero-temperature penetration depth comparable to the monocrystalline in-plane $\lambda = 0.14 \mu\text{m}$.²⁰ Since the fit is quite insensitive to changes of the parameters p_c and t , these two were kept fixed at the 2D bond percolation values $p_c = 0.5$ and $t = 1.3$ (Ref. 16) for all samples investigated. Thus, for the fit of $\Lambda^{-1}(T)$ in the critical region there are effectively only two adjustable parameters: R_{av} and δR , which were found to be 345 and 60 Ω , respectively. Notice that the theoretical curve correctly describes the divergence of Λ up to $\Lambda \sim 1 \text{ mm}$. Large-scale sample inhomogeneities and fluctuation effects are probably responsible for the observed rounding of the foot of the $\Lambda^{-1}(T)$ curve. The value found for R_{av} is slightly too large when compared with the measured dc sheet resistance of $R_{\square} = 250 \Omega$. In other samples the difference was even more pronounced, but always $R_{av} > R_{\square}$. This systematic discrepancy is possibly due to a reduction of the coupling energy caused by a lowering of the gap parameter Δ at the grain surfaces,⁴ which is equivalent to a smaller R_0 in Eq. (4), and hence to a smaller R_{av} in our analysis. Also shown in Fig. 2 is a dashed line corresponding to the universal KTB prediction $\Lambda(T_c)T_c = 19.6 \text{ mm K}$ for the value of Λ at the jump. In all samples investigated so far, the jump at T_c was at least a factor of 2 larger than expected for a KTB transition, thereby showing that the percolative transition occurs below the temperature regime dominated by fluctuation effects and providing an *a posteriori* justification for the use of Eq. (1). Moreover, calculations based on the

KTB recursion relations at nonzero frequencies^{17,21} always predict much sharper transitions than the observed ones.

Additional evidence for the percolation interpretation of the superconducting transition of YBCO films is, at least qualitatively, provided by an analysis of the dissipation present in the films below T_c . In almost all the samples investigated so far we have observed below the transition a monotonic increase of $\text{Re}\delta V$ with decreasing temperature, as shown by the $\text{Re}\delta V(T)$ curve of Fig. 1. In part, this effect is a measurement artifact: the temperature dependence of the resistances of the measuring coils, which causes a temperature-dependent variation of the phase angle in the detection system.¹³ Taking this effect into account in the analysis results in a small and negligible error in the determination of $\Lambda^{-1}(T)$, but results in an appreciable error in the $\text{Re}Z(T)$ curve. The absolute level of the $\text{Re}Z(T)$ curve shown in Fig. 3 is thus somewhat uncertain; however, with a noise floor of $\sim 0.1 \mu\Omega$, it clearly shows that there is a large temperature regime below the transition with nonvanishing dissipation. This is in qualitative agreement with the result of a Monte Carlo calculation of the frequency-integrated real part of the fluctuation conductivity of model granular superconductor,¹⁵ where dissipation below T_c was found to arise from the presence of disorder, possibly in the form of dangling bonds. The dissipation observed in our YBCO films below the transition region would then be the consequence of the percolation probability¹⁶ being less than unity, but slowly increasing with decreasing temperature, to finally reach unity at $\sim 50 \text{ K}$. This in turn implies that there are more (a few percent) high-resistance junctions than predicted by a Gaussian distribution with the mean and the standard deviation found above.

In a percolation description of the superconductive transition one would expect the initial rise of resis-

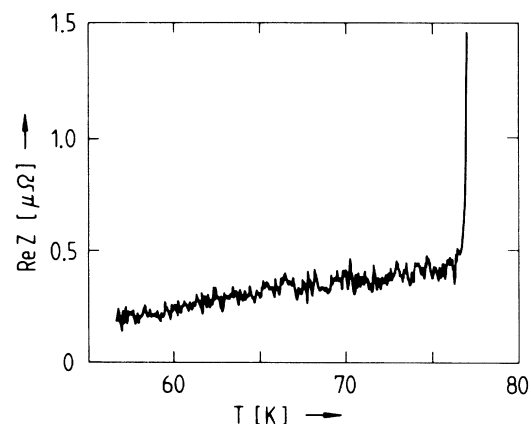


FIG. 3. $\text{Re}Z$ as a function of temperature deduced from the measurement of Fig. 1, showing non-negligible dissipation down to $\sim 50 \text{ K}$.

tance to be, at least approximately, given by $R_{\square}(T) \simeq R_{av} |p(T) - p_c|^l$. The resistive transitions of our YBCO films do not fit such an expression. This is probably due to a distribution of the single-grain transition temperatures T_{c0} and, more importantly, to the increasing importance of thermal fluctuations leading to effects such as phase slippage across grain boundaries²² and order-parameter amplitude fluctuations.²³ These effects dominate the resistive transition rendering the effect of percolative coupling between the grains secondary and observable only *below* T_c , where almost all the grains are superconducting and amplitude fluctuations frozen out. This is consistent with the observation that a percolation description of the resistive transition is successful in cases where the transition is split into two sections, with a tail extending into a temperature regime without order-parameter amplitude fluctuations.²⁴

In conclusion, both the attractive simplicity of the model presented in this paper and the excellent agreement between the predictions of the model and the measured temperature dependence of the penetration depth provide strong support for the description of the superconductive transition of YBCO films with a percolation model. We dismiss an interpretation of our data in terms of a vortex unbinding transition, since the observed jump in superfluid density at the transition is always too large and the transition region wider than expected. Unfortunately we are not able to verify that, as predicted by Ebner and Stroud,¹⁵ the exponent describing the divergence of Λ at the percolation threshold is indeed the conductivity exponent.

J. Weber's Rutherford backscattering spectroscopy measurements and analyses are gratefully acknowledged, as well as P. Debély's valuable technical assistance in the early stages of this project. This work was supported by the Swiss National Science Foundation.

^(a)Present address: Laboratorium für Festkörperphysik, Eidgenössische Technische Hochschule Zürich-Hönggerberg, 8093 Zürich, Switzerland.

¹T. K. Worthington, W. J. Gallagher, and T. R. Dinger, Phys. Rev. Lett. **59**, 1160 (1987).

²J. R. Clem, Physica (Amsterdam) **153-155C**, 50 (1988).

³R. L. Peterson and J. W. Ekin, Phys. Rev. B **37**, 9848 (1988).

⁴G. Deutscher and K. A. Müller, Phys. Rev. Lett. **59**, 1745 (1987).

⁵V. Ambegaokar and A. Baratoff, Phys. Rev. Lett. **10**, 486 (1963).

⁶J. M. Kosterlitz and D. J. Thouless, J. Phys. C **6**, 1181 (1973).

⁷A. T. Fiory, A. F. Hebard, P. M. Mankiewich, and R. E. Howard, Phys. Rev. Lett. **61**, 1419 (1988).

⁸S. Martin, A. T. Fiory, R. M. Fleming, G. P. Espinosa, and A. S. Cooper, Phys. Rev. Lett. **62**, 677 (1989).

⁹D. H. Kim, A. M. Goldman, J. H. Kang, and R. T. Kampwirth, Phys. Rev. B **40**, 8834 (1989).

¹⁰N.-C. Yeh and C. C. Tsuei, Phys. Rev. B **39**, 9708 (1989).

¹¹X. X. Xi, G. Linker, O. Meyer, and J. Geerk, J. Less-Common Met. **151**, 349 (1989).

¹²A. T. Fiory, A. F. Hebard, P. M. Mankiewich, and R. E. Howard, Appl. Phys. Lett. **52**, 2165 (1988).

¹³B. Jeanneret, J. L. Gavilano, G.-A. Racine, Ch. Leemann, and P. Martinoli, Appl. Phys. Lett. **55**, 2336 (1989).

¹⁴G. Deutscher, O. Entin-Wohlman, S. Fishman, and Y. Shapira, Phys. Rev. B **21**, 5041 (1980).

¹⁵C. Ebner and D. Stroud, Phys. Rev. B **28**, 5053 (1983).

¹⁶S. Kirkpatrick, Rev. Mod. Phys. **45**, 574 (1973).

¹⁷B. Jeanneret, Ph. Flückiger, J. L. Gavilano, Ch. Leemann, and P. Martinoli, Phys. Rev. B **40**, 11 374 (1989).

¹⁸M. R. Beasley, J. E. Mooij, and T. P. Orlando, Phys. Rev. Lett. **42**, 1165 (1979).

¹⁹M. Tinkham, *Introduction to Superconductivity* (McGraw-Hill, New York, 1975).

²⁰D. R. Harshman, L. F. Schneemeyer, J. V. Waszczak, G. Aeppli, R. J. Cava, B. Batlogg, L. W. Rupp, E. J. Ansaldo, and D. L. Williams, Phys. Rev. B **39**, 851 (1989).

²¹V. Ambegaokar, B. I. Halperin, D. R. Nelson, and E. D. Siggia, Phys. Rev. B **21**, 1806 (1980).

²²R. Gross, P. Chaudhari, D. Dimos, A. Gupta, and G. Koren, Phys. Rev. Lett. **64**, 228 (1990).

²³D. H. Kim, A. M. Goldman, J. H. Kang, K. E. Gray, and R. T. Kampwirth, Phys. Rev. B **39**, 12 275 (1989).

²⁴C. J. Lobb, M. Tinkham, and W. J. Skocpol, Solid State Commun. **27**, 1273 (1978).